Journal of Population Therapeutics & Clinical Pharmacology

RESEARCH ARTICLE
DOI: 10.53555/jptcp.v30i17.2900

PHYTOCOMPOUND-BASED DRUG DISCOVERY APPROACH TO EXPLORE THE FROSTBITE HEALING POTENTIAL OF ABIETADIENE ISOLATED FROM *PINUS ROXBURGHII*

Hasan Akbar Khan[1], Asma Ahmed[2*], Khadija Kiran[3], Samra Hafeez[4], Rehana Badar[5], Sajjad Ahmad[6]

[1,2*,4,5]Institute of Molecular Biology and Biotechnology (IMBB), The University of Lahore, Lahore, Pakistan
[3]Department of Physiology, Gujranwala Medical College, Gujranwala, Punjab, Pakistan
[5]Department of Biological Sciences Superior University Lahore Punjab, Islamic Republic of Pakistan
[6]Department of Health and Biological Sciences, Abasyn University, Peshawar, Pakistan

***Corresponding Author:** Asma Ahmed
Email: asma.ahmed@imbb.uol.edu.pk

Abstract
Exposure to subzero temperatures usually leads to vascular damage causing severe ischemic injury known as frostbite, one of the prominent cold weather injuries that can lead to devastating consequences such as amputation of the extremities. Although rate of amputation due to frostbite has decreased recently due to thrombolytic therapy but this new regimen comes with a price as well which include symptoms such as profuse gastrointestinal bleeding in patients. Thus, there is a need to discover effective treatments with least side effects and more bioavailability rate. In current work, aqueous extract of *Pinus roxburghii* leaves were checked against dry-ice induced frostbite on plantar surfaces of albino Wistar rats (both genders, 150-200 g) by keeping heparin as control, followed by the computational evaluation of its phytocompounds to prioritize potential antiinflammatory and anti-thrombotic compounds against frostbite. Statistically analyzed results of molecular docking showed that among all secondary metabolites of *P.roxburghii*, abietadiene was most suitable potential ligand against antiplasmin and antithrombin III, which modulated anticoagulant pathway and proved to be a valuable anti-inflammatory and antithrombotic agent for wound healing. These results suggest the wound healing potential of abietadiene especially in case of frost bite which further needs to be validated experimentally.

1. INTRODUCTION

Cold weather injuries or CWIs may affect central nervous system (as in hypothermia) or the peripheral regions of the body (in case of frostbite). The injuries that principally affect the peripheral regions of the body are further classified into freezing and non-freezing cold injuries. Freezing cold injuries are characterized by damage which occurs due to exposure to temperatures below freezing point i.e. -0.55 °C [1]. Whereas, non-freezing cold injuries are identified by a gradual decline in the tissue temperature without direct freezing [2]. Frostbite is a type of freezing cold injuries and occurs after flesh is exposed to temperatures below freezing point for a considerable amount of time [3]. Three hallmark characteristics of a frostbite injury include tissue inflammation due to ice crystals formation

in intracellular and extracellular compartments; dehydration in intracellular compartment and last but certainly not the least ischemia, which occurs because of intravascular thrombosis. Predominantly, extremities such as digits of hands and feet are affected, albeit, the injury can progress to nose, cheeks and ears as well[4]. Serious cases of frostbite can lead to severe debilitating injuries which include amputation of the affected part [5]. Researchers have found out that the administration of thrombolytic therapy can substantially hamper the incidences of amputation if or when administered within 24 hours of frostbite injury [6]. Therefore, severe cases of frost bite are now managed with the administration of tissue plasminogen activator and this has shown potential to drastically reduce the rate of amputation in patients [7]. A newly conducted study has shown promising results of reduced rates of amputation with a drug regimen of iloprost, alteplase and heparin [7]. While Iloprost is a prostacyclin (PGI_2) analogue[8], Alteplase is a recombinant tissue plasminogen (t-PA) activator [9], and Heparin accomplishes thrombolysis by binding to antithrombin III and augmenting its actions [10]. All of the aforementioned medications bring along their baggage of deleterious side effects and increase the potency when used in conjunction with each other. Iloprost, if given individually, exhibits mild side effects such as flushes and headaches [11], but probability of its hazardous side effects such as profuse bleedingare increased if given in conjunction with anticoagulants as it then interferes with the normal functioning of platelets [12]. On the other hand, Tissue plasminogen activator (t-PA) or its synthetic forms such as alteplase have been documented to upregulate matrix-metalloproteinases-9 (MMP-9) [13,14]. These MMP-9s are involved in the degeneration of connective tissue such as collagen and various other matrix proteins that constitute the blood-brain barrier [15,16]. This results in severe side effects such as cerebral bleeding, swelling of the brain and neurotoxicity [17].Lastly, heparin has its own set of adverse effects which include thrombocytopenia, allergic reactions, bleeding and raised levels of transaminase [18].

Thrombosis is usually described as blood clotting inside a blood vessel induced by either an irregularity in platelets or a protein that helps in the coagulation of blood [19]. This deformity promotes vascular stenosis which results in decreased blood perfusion of the affected tissue [20]. Thrombosis can have a devastating medical effect and is the leading cause of myocardial infarction in majority of developed countries [21]. Acute management of any thrombus is essential as if thrombus is not removed it will lead to tissue ischemia and necrosis of the tissue supplied by that particular vessel [22]. Current management of thrombosis encompasses antithrombotic medications which categorically target proteins participating in coagulation pathways. 'Though various medications are available against thrombosis but few of these drugs are incriminated with instigating profuse bleeding when administered to the patient [23].Also, gastrointestinal bleeding accounts for one of the major side effects of these medications [24]. Thus, to increase the specificity and selectivity and also to minimize the profound side effects of the earlier anticoagulants and their fabricated derivatives e.g. coumarins and heparins, there is a need to increase the safety profile of such drugs which usually can be achieved by targeting phytoconstituents of anti-inflammatory and anti-thrombotic plants [25].

Comprehension and utilization of plants as nutritional and medicinal sources have been accomplished through hits and misses. But little by little, humans have enabled themselves to dot the i's and cross the t's [26]. Presently, bioactive compounds of plants are gaining immense limelight because of their better nutritional productiveness, safety and promising pharmacodynamics [27]. Pure unrefined medications derived from plants have been conventionally employed as anti-thrombotic drugs by almost all indigenous people of our planet [28]. Numerous phytochemicals and secondary metabolites have been found in plants which play a role in the *in vivo* and *in vitro* degradation of clots 29,30. Psychrophytes are defined as "Any plant that tolerates, or thrives in a cold climate, especially in arctic or alpine conditions". These plants thrive under climates where the average annual temperature remains constantly below the freezing point of water i.e. 0 °C and thus have been extensively used in folklore due to their far-reaching medicinal abilities [3132–36]. *Pinus roxburghii* Sarg (Chir pine), is considered as an eminent local species [37]. It is distributed in the regions varying from 900 to 1800 meters above sea level [38]. In Pakistan, *P.roxburghii* is found in Azad Kashmir, Khyber Pakhtunkhwa and some parts of Punjab [39]. Five types of *P.roxburghii*occur in Pakistan with total span of them being

1928 thousand hectares of land [40]. Outside of its conventional medicinal usage, numerous other biomedical functions of *P.roxburghii* have been studied which include antioxidant [41], anti-inflammatory [42], antiparasitic [43], anticancer [44], antimicrobial [45], antihyperlipidemic and antioxidant properties [46] . In this study, we have studied all the phytocompounds of *P.roxburghii*and evaluated their antithrombotic potential by pitting them against modulators ofClotting cascade (**Table 1**).

Conventional screening methods employed for drug designing and drug discovery are very costly, takes immense amount of time to perform and are not effective enough to discover avant-garde drugs which could be used in therapeutics [47]. Thus, in this study *in silico*methods have been employed to identify potential phytoconstituents responsible for wound healing activity of *P.roxburghii*and to determine their potential anti-thrombotic and anti-inflammatory properties.

2. METHODOLOGY

Plant collection, identification **and extract preparation** Plants were collected in triplicates from Minimerg, Pakistan, and then stored at -80 °C to protect them from stress, followed by their identification by the expert botanist atDepartment of Botany, The Government College University, Lahore, Pakistan. Leaves and roots of identified plants were separated and washed with ethanol. Aqueous extract of plants have been prepared by modifying the protocol of Asma et al. , (2016) and Bashir et al. , 2018. Collected supernatants were left at room temperature for evaporation and extracts were then stored at -80 °C. (**Table 1**).

Animal Models

Whole experiment has been performed in triplicate at the Institute of Molecular Biology and Biotechnology (IMBB), The University of Lahore, Lahore, Punjab, Pakistan, after approval from the ethical committee ethical approval(Approval No: USM/Animal Ethics approval/2009/[45] [140] on albino Wistar rats (both genders) of 150-200 g in stainless steel restrainer boxes, at controlled temperature (18-26°C) and humidity (40-60 %) with free access to food (poultry feed no. 1) and water.Animals were grouped as vehicle (No induction of dry ice, heparin and plant extract), Negative control (dry ice induced only), Positive control (Dry ice induced inflammation, followed by induction of heparin as positive anti-inflammatory control) and Experimental groups (Dry ice induced inflammation, followed by induction of plant extracts).

Screening of plant extracts as thrombolytic agents

Rats in negative control, positive control, and experimental groups were anesthetized with 0.4 cc intraperitoneal Ketamine injection, followed by the application of dry ice for 30 seconds on plantar surfaces of the hind paws of rats which instigated the formation of inflammation [48]. With the use of 1 cc syringes, 0.6 cc of 1.0 mg/mL plant extracts (both leaf and root) were injected after one day of dry ice application on the plantar surface of the rat hind foot in each experimental group, while 450 IU/Kg of Heparin (5000IU/ml) was injected subcutaneously in hind paw of positive control group.The rats' paw thickness was measured in centimeters using a pre-calibrated Vernier caliper for ten consecutive days[49]. During the trial, the animals were checked daily for changes and indicators of toxicity. Paw thickness has been calculated by using following formula; Paw thickness before application of dry-ice= A(cm) Every subsequent measurement was noted after subtracting value of A After 10 days, rats (both treated and controlled) were sacrificed afterbeing anesthetized by Ketamine injection to take skin samples from plantar surfaces of all the rats in formalin solutionfor preservation. 3-4 µm thick histological crosssections were made after fixation which were then stained with hematoxylin and eosin (H & E) and examined under microscope at 40X. In histological examination,scoring system mentioned by Abramov [50] was used for checking the extent of wound healing.

Compound identification and selection

For ligands selection, structural information about the bioactive compounds of leaves and root extracts of*P.roxburghii*was retrieved [51–55], followed by the evaluation of compounds for their druglikeness based on Lipinski's rule[56,57]and ADMET propertiesthrough SwissADME server [58]. 3D structures of selected compounds were obtained from PubChem[59]. For receptors selection, FASTA sequences of intermediary compounds which modulate the anticoagulant pathway were obtained from Uniprotof *Homo sapiens*[60] and their 3D structures were obtained from Swiss-model [61]. Best model obtained was selected on the basis of GMQE (Global Model Quality Estimation), QMEAN (Qualitative Model Energy Analysis), coverage and sequence identity [61]. Models were protonated,tethered, and unbound water molecules were deleted usingChimera 1.15[62]. Then energies of pdb structures of both ligands and receptors were minimized by Chiron [63].

All selected compounds were then docked with receptors using CB dock[64]. COACH server [65] and SPPIDER [66] were used to find interacting residues. Docked complexes were then correlated with Ligplot[67] to find the actual binding residues of ligand with receptor proteins.

Molecular Dynamics Simulations

Constrained ESP (RESP) charges were bred by employing Antechamber module of AMBER v.20 [68] on best binding modes of all of the ligands. AMBER ff14SB force field was utilized for parameterization of the proteins, whereas rest of the parameters were extracted from AMBER ff14SB force field [68]. LEAP module of AMBER v.20 was applied for ion additions and solvation of complexes in which acetylcholinesterase enzymes and ligands were present. Water boxes subsisting of small TIP3P (TIP3PBOX) were used to enclose protein-ligand complexes. 10 A° distance was set between the solute surface and outer boundary of the solvent box. SANDER modules of AMBER v.20 were used for the implementation of temperature and relaxation equilibration of the solvated complexes. PMEMD.CUDA module of AMBER v.20 running at Turkish TR-Grid eInfrastructure was adopted for molecular dynamic (MD) computations. Steps carried out consisted of solvation, relaxation (500 steps), minimization (500 steps), heating (10ps), and MD simulation (300 ns). The aforementioned steps were carried out under previously optimized protocols [68].

Post-trajectory Analysis

CPTRAJ module of AMBER v.20 was adopted for analysis of hydrogen bond formation and root mean square deviation (RMSD) values acquired after MD simulations [68]. Mass-weighted RMSD was utilized in the current study and in order to comprehend the extent of deviation of structure from its primary configuration, the input coordinate file received following minimization process, was employed as a reference. Hydrogen bond arrangement of complexes was evaluated throughout the trajectories. Chimera molecular modeling program was used for evaluating 300 ns binding profile in the trajectory files [68]

Binding free energy analysis

MM-GBSA (Molecular Mechanics-Generalized Born Surface Area) and Molecular Mechanics Poisson Boltzmann Surface Area (MM_PBSA) modules of AMBER v.20 were employed for computations of binding energies of ligands in complex with acetyl cholinesterase enzyme [68]. Poisson Boltzmann and Generalized Born procedures were adopted for MM_PBSA calculations (igb = 5) with salt concentration being 0.15 M. Fill ration and ionic strength values are calculated as 4.0 and 0.15 respectively. Interior dielectric constant was set at the default value of 1.0. Binding energy has been expressed here as: $\Delta G_{binding} = E_{MM} + \Delta G_{solv} - TS$.

Alteration in the free energy (ΔG binding) of every individual system were determined with the aid of molecular mechanics' energy (EMM) of the system in gaseous phase (ΔG gas) in addition to entropy (S) and molecular mechanics' energy (EMM) (ΔG solv) at a particularized temperature T.

Entropic contribution in a vacuum is denoted by TS. The equation used for calculations was: $\Delta G_{binding} = \Delta G_{AS} + \Delta G_{solv}$.

ΔGgas is obtained after addition of internal energy (Eint) with van der Waals energy (Evdw) and electrostatic energy (Eelec). The abovementioned energies emanate as a result of dihedral, bond and angle interactions. Eint determined zero when single trajectory approach was adopted. ΔGsolv is obtained as sum total of non-electrostatic free energy of solvation (Gnonpol), dispersion energy (Gdisperse), and electrostatic energy of solvation (Gpol).

3. RESULTS

3.1 Thrombolytic activity

Vehicle showed no paw thickness (zero-centimeter thickness to male and females respectively) whileno reduction in paw thickness was observed in negative control group and injury increased with the passage of time (Paw thickness before experiment was 1.3±0.01cm in female and 1.28±0.02 cm in male). The change of injury in negative control group had been observed on the day one (3.3±0.04 cm in female and 3.1±0.06 in male), while reduction in paw thickness on day 10 was3.28±0.05 and 3.2±0.06 in female and male respectively**.** Positive control group showed significant reduction in the thickness from day 3 to onwards till day 10 (Paw thickness before experiment was 1.3±0.04 cm in female and 1.32±0.05 in male). However, the reduction of injury in positive control group on day one after treatment was 0.8±0.02 cm in female and 0.7±0.01 in male. Furthermore, the reduction on day 10 in female and male was 0.3±0.09 and 0.2±0.08 respectively.Paw thickness before application of extracts of *P.roxburghii*(GC Herb. 3754) was 1.32±0.02cm and 1.3±0.04, which significantly ($p<0.0001$) reducedafter applying leave extract (from 2.76±0.05 cm and 2.8±0.02 on day 1 of application of extracts to 0.7±0.01 cm and 1.05±0.02 on the 10^{th} day) in female and male rats respectively. Moreover, in the case of root extract, paw thickness before experiment was 1.32±0.06cm in female and 1.3±0.02 in male. It showed reduction from 2.6 ±0.01 and 2.9±0.01 cm on day 1 of application of extracts to 1.18±0.01 cm and 1.1±0.01 in female and male rats respectively on the 10^{th} day (Table 1).

3.2 Histopathological Examination of Paw Skin

Histology reported according to wound healing histological criterion of Abramov [50] at 40 X showed that maleand female skin of vehicle showed no signs of acute or chronic inflammation. While male skin showed mild re-epithelization and granulation tissue formation along with abundant collagen deposition and thorough granulation tissue maturation, with mild neovascularization and female skin showed dense reepithelization and partial granulation tissue formation was seen along with abundant collagen deposition and moderate granulation tissue maturation, while neovascularization was absent{Figure 1.(a, b)}.Histological examination of male and female rat skin of positive control groups showed dense signs of acute inflammation, partial reepithelization and granulation tissue formation along with limited collagen deposition and granulation tissue maturation, with absence of chronic inflammation and neovascularization{Figure 1 (c, d)}.Histological examination of male rat skin innegative controlgroup showed moderate signs of acute inflammation with absence of chronic inflammation, while female rat skin showed signs of heavy acute and limited chronic inflammation. Reepithelization, limited granulation tissue formation and maturation with collagen deposition and neovascularization have been observed in skin of both male and female rats {Figure 1 (e, f)}.Histological examination ofmale and female rat skin after application of leave and root extracts of *P.roxburghii* showed no signs of acute inflammation but signs of mild chronic inflammation was observed. After application of leave extracts, skin of male rat had dense reepithelization with no granulation tissue formation along with moderate collagen deposition, fibroblast maturation and with neovascularization of up to 5/HPF (High power field). Whereas, skin of female rats showed limited reepithelization with partial granulation tissue formation along with mild collagen deposition and fibroblast maturation, with absence of neovascularization{Figure 1 (g, h)}. After application of root extracts only, intermediate reepithelization with partial granulation tissue formation was seen along with moderate collagen deposition and fibroblast maturation, with neovascularization of up to 5/HPF in skin of male rats. Whereas,signs of modest acute inflammation and mild chronic inflammation,

with moderate reepithelization and granulation tissue formation was seen along with moderate collagen deposition and fibroblast maturation and neovascularization of up to 6-10/HPF in skin of female rats {Figure 1 (i, j)}.

Table 1 Experimental data of thrombolytic effect of *P.roxburghii* extracts against coldinduced injury in albino rats indicated by changes in paw thickness measured in centimeters for ten days

Groups	Extracts	Gender	Paw thickness in cm/ Days										
			Before application of dry ice (A)	After application of dry ice**	After application plant extract/ Heparin**								
			Zero	One	Two	Three	Four	Five	Six	Seven	Eight	Nine	Ten
Vehicle control	Distilled Water	F	1.3	0±0	0±0	0±0	0±0	0±0	0±0	0±0	0±0	0±0	0±0
		M	1.3	0±0	0±0	0±0	0±0	0±0	0±0	0±0	0±0	0±0	0±0
Negative control	N/A	F	1.3	3.3±0.04	3.72±0.05	3.9±0.08	3.1±0.05	3.32±0.05	3.28±0.06	3.28±0.04	3.28±005	3.28±0.03	3.28±0.05
		M	1.28±0.02	3.1±0.06	2.82±0.06	2.5±0.08	3.12±0.04	3.36±0.08	3.42±0.09	3.38±0.03	3.4±0.05	3.4±0.06	3.2±0.06
Positive control	Heparin	F	1.3±0.03	0.9±0.02	0.7±0.03	0.5±0.02	0.4±0.06	0.3±0.05	0.3±0.06	0.3±0.08	0.35±0.06	0.3±0.05	0.3±0.09
		M	1.32±0.04	0.8±0.01	0.6±0.01	0.3±0.04	0.±0.08	0.2±0.05	0.3±0.01	0.2±0.05	0.2±0.06	0.2±0.08	0.2±0.08
P.roxburghii	L	F	1.32±0.02	2.76±0.05	2.2±0.03	1.7±0.3	2±0.01	2±0.01	2.1±0.01	1.9±0.02	1.5±0.01	1.1±0.01	0.7±0.01
	R	F	1.32±0.06	2.6±0.01	2.4±0.01	2.1±0.01	1.9±0.02	2±0.03	1.9±0.01	2.1±0.02	1.7±0.01	1.3±0.02	1.18±0.01
	L	M	1.3±0.04	2.8±0.02	2.5±0.03	2.1±0.02	2±0.05	1.8±0.04	1.4±0.03	2.0±0.02	1.6±0.02	1.2±0.01	1.1±0.01
	R	M	1.3±0.02	2.9±0.01	2.5±0.02	2.4±0.05	2.1±0.03	2.05±0.02	1.4±0.04	1.7±0.04	1.3±0.01	1.1±0.03	1.05±0.02

Where; F: Female Albino wistar rats; **M**: Male Albino wistar rats; **N/A**: nothing was administered; **L**: extracts of leaves of *P.roxburghii*;**R**: extracts of roots of *P.roxburghii*

A= Paw thickness before the start of experiment **= Values are mentioned after subtracting values of A

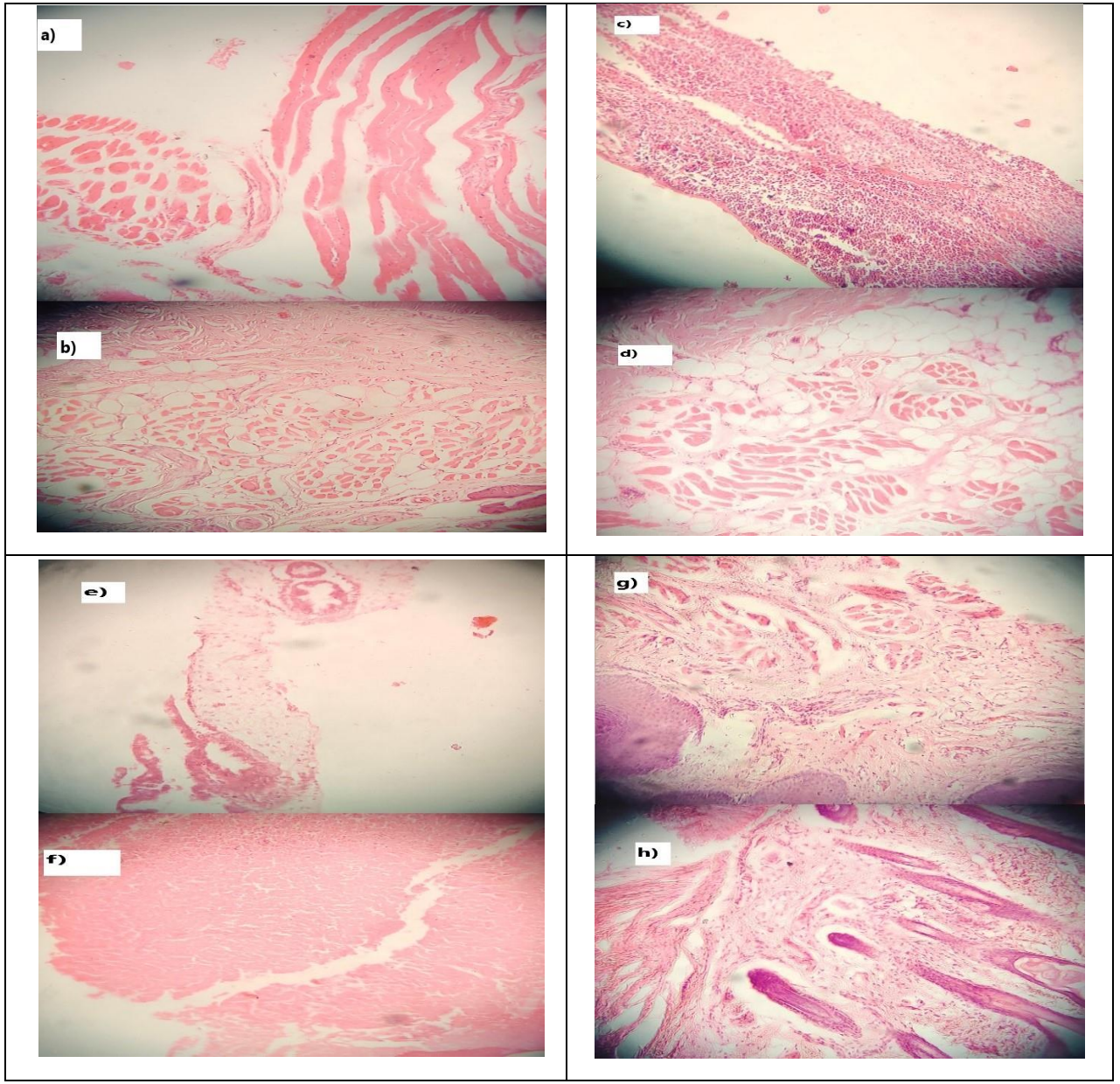
a)
b)
c)
d)
e)
f)
g)
h)

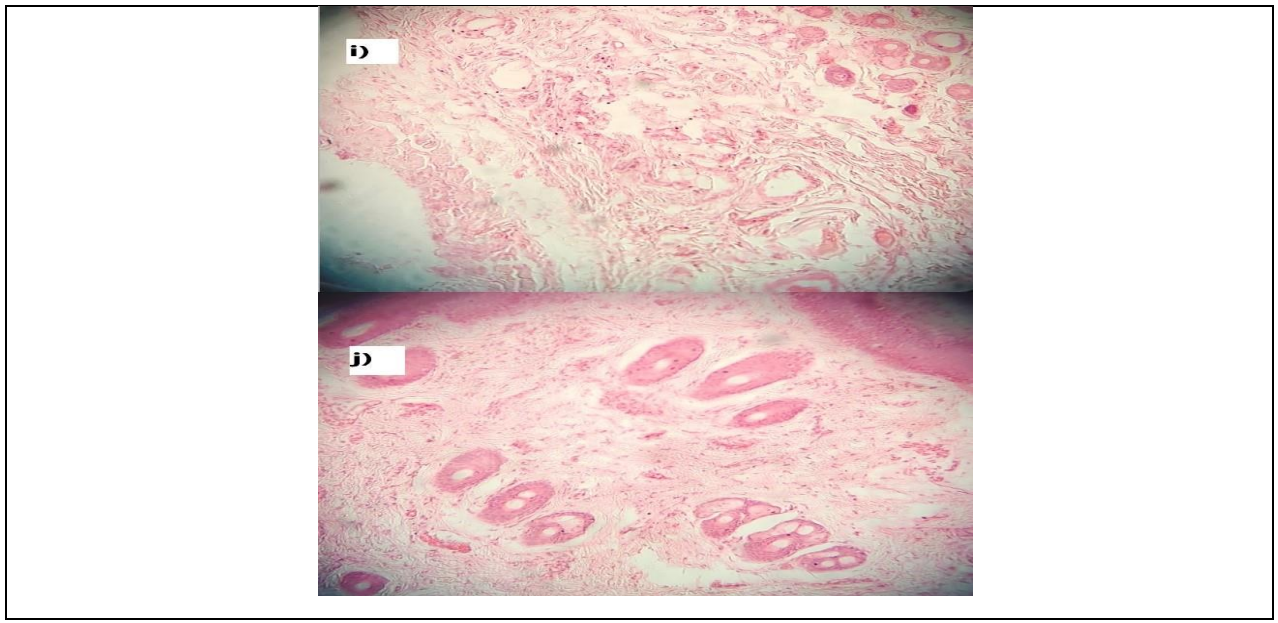

Figure 1: Histopathology at 40X of (a) Male (b) Female vehicle. (c) Male and (d) female Positive control group. (e) Male (f) female Negative control group. (g) Male and (h) female Experimental groups treated with leaf extract of *P.roxburghii*.(i) Male and (j) Female Experimental group treated with root extract of *P.roxburghii*

3.3 Ligand Selection

Selected secondary metabolites of *P.roxburghii* found through literature were filtered through ADMET studies and Lipinski's rule through SwissADME server [58]. Seven compounds have been selected with drug-likeness properties and thus were further subjected for interaction analysis with potential host receptors(**Table 2**).

3.4 Virtual Screening

Secondary metabolites *P.roxburghii* including carene, copaene, abietadiene, humulene, italicene, juvabione, sandaracopimarinal and scalene were docked against modulators of anticoagulant pathway i.e. α2-antiplasmin, antithrombin III, plasminogen activation domain, plasminogen activation inhibitor 1, plasminogen activation inhibitor 2, protein C, Urokinase Plasminogen activator and Urokinase Plasminogen activator surface protein. On the basis of binding energies of best docked complexes with selected ligands (**Table 3),** abietadieneshowed best interaction with antithrombin III and α2-antiplasmin (α2-AP). The binding energy of best model of abietadiene with α2AP was -6.2 kcal/mol while the binding energy best model ofAbietadiene with antithrombin III was -8.1 kcal/mol **(Figure 2).**

Table 2: *In silico* analysis of selected secondary metabolites of *P. roxburghii* using SwissADME server [58]

Properties/ Compounds and their values	Abietadiene	Copaene	Humulene	Italicene	Juvabione	Sandaracopimarinal	Sclarene	Carene
PHYSICOCHEMICAL PROPERTIES								
Formula	$C_{20}H_{36}$	$C_{15}H_{26}$	$C_{15}H_{30}$	$C_{15}H_{24}$	$C_{16}H_{28}O_3$	$C_{20}H_{30}O$	$C_{20}H_{32}$	$C_{10}H_{16}$
Molecular Weight (g/mol)	308.75	230.56	234.59	228.54	294.60	286.45	272.47	136.23
Number of heavy atoms	20	15	15	15	19	21	20	10
Number of aromatic heavy atoms	0	0	0	0	0	0	0	0
Fractions Csp3	1	1	1	1	0.88	0.75	0.7	0.8
Number of rotatable bonds	1	1	0	0	7	2	4	0
Num. H-bond acceptors	0	0	0	0	3	1	0	0
Num. H-bond donors	0	0	0	0	0	0	0	0
Molar Refractivity	91.39	67.62	71.84	64.72	78.4	90.38	92.08	45.22
TPSA (A^O)	0.00	0.00	0.00	0.00	43.37	17.07	0.00 ²	0.00
LIPOPHILICITY								
Log Po/w (iLOGP)	0	0	0	0	0	3.44	4	2.63
Log Po/w (XLOGP3)	8.08	5.52	7.11	5.15	3.63	5.48	7.5	4.38
Log Po/w (WLOGP)	9.9	7.05	8.12	6.95	6.53	5.32	6.31	3
Log Po/w (MLOGP)	6.99	5.8	5.8	5.8	2.81	4.65	5.72	4.29
Log Po/w (SILICOS-IT)	5.26	3.74	4.34	4.3	3.75	5.21	6.17	2.79
Consensus Log Po/w	6.05	4.42	5.07	4.44	3.34	4.82	5.94	3.42
WATER SOLUBILITY								
Log S (ESOL)	-6.78	-4.68	-5.77	-4.5	-3.49	-4.94	-5.99	-3.44
Solubility	5.14e-05 mg/ml; 1.66e-07 mol/l	4.81e-03 mg/ml ; 2.08e-05 mol/l	3.95e-04 mg/ml ; 1.68e-06 mol/l	7.20e-03 mg/ml ; 3.15e-05 mol/l	9.50e-02 mg/ml ; 3.23e-04 mol/l	3.32e-03 mg/ml ; 1.16e-05 mol/l	2.79e-04 mg/ml ; 1.02e-06 mol/l	4.90e-02 mg/ml ; 3.60e-04 mol/l
Class	PS	MS	MS	MS	S	MS	MS	S
Log S (Ali)	-7.94	-5.28	-6.93	-4.9	-4.23	-5.6	-7.33	-4.1
Solubility	3.58e-06 mg/ml; 1.16e-08 mol/l	1.21e-03 mg/ml ; 5.26e-06 mol/l	2.76e-05 mg/ml ; 1.18e-07 mol/l	2.91e-03 mg/ml ; 1.27e-05 mol/l	1.74e-02 mg/ml ; 5.90e-05 mol/l	7.26e-04 mg/ml ; 2.53e-06 mol/l	1.26e-05 mg/ml ; 4.64e-08 mol/l	1.09e-02 mg/ml ; 8.01e-05 mol/l
Class	PS	MS	PS	MS	MS	MS	PS	MS
Log S (SILICOS-IT)	-4.8	-3.09	-4.03	-3.97	-3.18	-4.57	-5.42	-2.23
Solubility	4.86e-03 mg/ml; 1.57e-05 mol/l	1.88e-01 mg/ml ; 8.17e-04 mol/l	2.21e-02 mg/ml ; 9.44e-05 mol/l	2.45e-02 mg/ml ; 1.07e-04 mol/l	1.94e-01 mg/ml ; 6.59e-04 mol/l	7.67e-03 mg/ml ; 2.68e-05 mol/l	1.03e-03 mg/ml ; 3.78e-06 mol/l	8.06e-01 mg/ml ; 5.92e-03 mol/l
Class	MS	S	MS	S	S	MS	MS	S
PHARMACOKINETICS								
GI Absorption	Low	Low	Low	Low	High	High	Low	Low
BBB permeant	No	No	No	No	No	Yes	No	Yes
P-gp substrate	Yes	No	No	Yes	No	No	No	No
CYP1A2 inhibitor	No	Yes	No	Yes	No	No	No	No
CYP2C19 inhibitor	No	Yes	No	Yes	No	Yes	Yes	No
CYP2C9 inhibitor	No	No	No	No	No	Yes	Yes	Yes
CYP2D6 inhibitor	No	No	No	No	No	No	No	No
CYP3A4 inhibitor	No	No	No	No	No	No	No	No
Log K_p(skin permeation)	-2.45 cm/s	-3.79 cm/s	-2.68 cm/s	-4.04 cm/s	-5.52 cm/s	-4.16 cm/s	-2.64 cm/s	-4.02 cm/s
DRUGLIKENESS								
Lipinski	Yes; 1 violation: MLOGP>4.15	Yes; 1 violation: MLOGP>4.15	Yes; 1 violation: MLOGP>4.15	Yes; 1 violation: MLOGP>4.15	Yes; 0 violation	Yes; 1 violation: MLOGP>4.15	Yes; 1 violation: MLOGP>4.15	Yes; 1 violation: MLOGP>4.15
Ghose	No; 2 violations: WLOGP>5.6, #atoms>70	No; 1 violation: WLOGP>5.6	No; 1 violation: WLOGP>5.6	No; 1 violation: WLOGP>5.6	No; 2 violations: WLOGP>5.6, #atoms>70	Yes	No; 1 violation: WLOGP>5.6	No; 1 violation: MW<160
Veber	Yes	Yes	Yes	Yes	Yes	Yes	Yes	Yes
Egan	No; 1 violation: WLOGP>5.88	No; 1 violation: WLOGP>5.88	No; 1 violation: WLOGP>5.88	No; 1 violation: WLOGP>5.88	No; 1 violation: WLOGP>5.88	Yes	No; 1 violation: WLOGP>5.88	Yes
Muegge	No; 2 violations: XLOGP3>5, Heteroatoms <2	No; 2 violations: XLOGP3>5, Heteroatoms<2	No; 2 violations: XLOGP3>5, Heteroatoms<2	No; 2 violations: XLOGP3>5, Heteroatoms<2	Yes	No; 2 violations: XLOGP3>5, Heteroatoms<2	No; 2 violations: XLOGP3>5, Heteroatoms<2	No; 2 violations: MW<200, Heteroatoms<2
Bioavailability score	0.55	0.55	0.55	0.55	0.55	0.55	0.55	0.55
MEDICINAL CHEMISTRY								
PAINS	0 alert	0 alert	0 alert	0 alert	0 alert	0 alert	0 alert	0 alert
Brenk	0 alert	0 alert	0 alert	0 alert	0 alert	2 alerts: aldehyde, isolated_alkene	2 alerts: isolated_alkene, polyene	1 alert: isolated_alkene
Leadlikeness	No; 1 violation: XLOGP3>3.5	No; 2 violations: MW<250, XLOGP3>3.5	No; 2 violations: MW<250, XLOGP3>3.5	No; 2 violations: MW<250, XLOGP3>3.5	No; 1 violation: XLOGP3>3.5	No; 1 violation: XLOGP3>3.5	No; 1 violation: XLOGP3>3.5	No; 2 violations: MW<250, XLOGP3>3.5
Synthetic accessibility	5.22	5.03	4.16	5.98	4.29	4.73	4.21	3.84

Poorly soluble= PS, Moderately soluble= MS, S= Soluble

Table 3: Docking of Secondary metabolites of *Pinus roxburghii* with modulators of anticoagulant pathway

Ligand	Receptor	Binding energy (kcal/mol)
Abietadiene	α2-Antiplasmin	-6.2
	Antithrombin III	-8.1
	Plasminogen Activation Domain	-8.6
	Plasminogen Activation Inhibitor 1	-8.5
	Plasminogen Activation Inhibitor 2	-7.5
	Protein C	-7.4
	Urokinase Plasminogen Activator	-7.1
	Urokinase Plasminogen Activator Protein Surface	-8.2
Copaene	α2-Antiplasmin	-5.9
	Antithrombin III	-7
	Plasminogen Activation Domain	-7.3
	Plasminogen Activation Inhibitor 1	-7.3
	Plasminogen Activation Inhibitor 2	-5.8
	Protein C	-5.9
	Urokinase Plasminogen Activator	-6.1
	Urokinase Plasminogen Activator Protein Surface	-6.8
Humulene	α2-Antiplasmin	-5.7
	Antithrombin III	-7
	Plasminogen Activation Domain	-6.7
	Plasminogen Activation Inhibitor 1	-7.4
	Plasminogen Activation Inhibitor 2	-5.2
	Protein C	-5.7
	Urokinase Plasminogen Activator	-6
	Urokinase Plasminogen Activator Protein Surface	-6.2
Italicene	α2-Antiplasmin	-2.1
	Antithrombin III	-2.8
	Plasminogen Activation Domain	-2.6
	Plasminogen Activation Inhibitor 1	-2.8
	Plasminogen Activation Inhibitor 2	-2.9
	Protein C	-2.7
	Urokinase Plasminogen Activator	-2.5
	Urokinase Plasminogen Activator Protein Surface	-2.6
Juvabione	α2-Antiplasmin	-5.7
	Antithrombin III	-6.5
	Plasminogen Activation Domain	-6.2
	Plasminogen Activation Inhibitor 1	-6.4
	Plasminogen Activation Inhibitor 2	-7.4
	Protein C	-6
	Urokinase Plasminogen Activator	-6.6
	Urokinase Plasminogen Activator Protein Surface	-6.6
Sandaracopimarinal	α2-Antiplasmin	-6.5
	Antithrombin III	-7.5
	Plasminogen Activation Domain	-7.1
	Plasminogen Activation Inhibitor 1	-8
	Plasminogen Activation Inhibitor 2	-6.7
	Protein C	-6.6
	Urokinase Plasminogen Activator	-6.6
	Urokinase Plasminogen Activator Protein Surface	-8.2
Sclarene	α2-Antiplasmin	-5.8
	Antithrombin III	-7.9
	Plasminogen Activation Domain	-7
	Plasminogen Activation Inhibitor 1	-8
	Plasminogen Activation Inhibitor 2	-6.8
	Protein C	-6.4
	Urokinase Plasminogen Activator	-6.2
	Urokinase Plasminogen Activator Protein Surface	-7.1
Carene	α2-Antiplasmin	-4.9
	Antithrombin III	-5.6
	Plasminogen Activation Domain	-5.7
	Plasminogen Activation Inhibitor 1	-6.1
	Plasminogen Activation Inhibitor 2	-6
	Protein C	-5.4
	Urokinase Plasminogen Activator	-5
	Urokinase Protein Plasminogen Activator Surface	-5.4

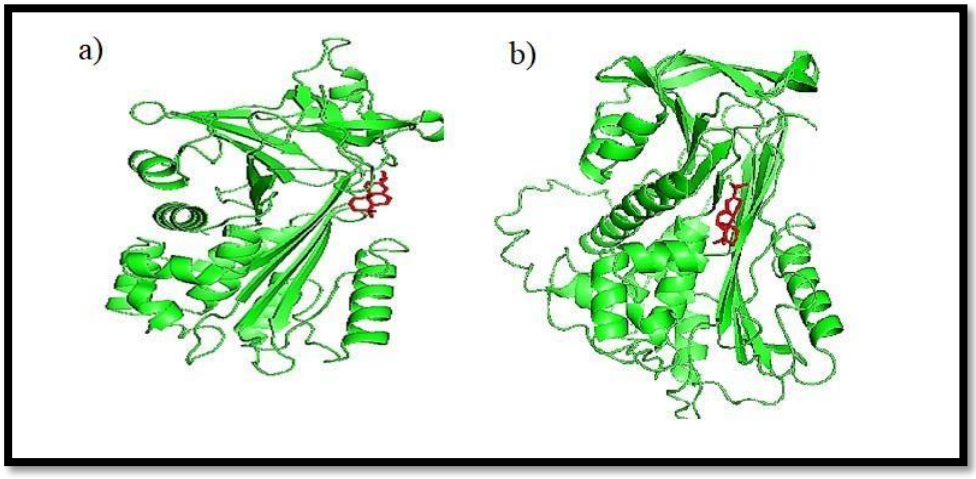

Figure 2: Molecular Docking of Abietadiene with (a) α2-Antiplasmin(-6.2 kcal/mol) and (b) Antithrombin III (-8.1 kcal/mol)

3.5 Interacting Residues

COACH and SPPIDER servers[65,66] were used to find the active binding site residues of Antithrombin III and α2- Antiplasmin (**Table 4**).

Table 4: Active binding site residues of α2- Antiplasmin and Antithrombin

S. No.	Protein	Active Binding Residues
1.	α2- Antiplasmin	1,5,10,163,231,247,257,284,311,312,313,392,396,398
2.	Antithrombin III	29,30,185,186,236,237,340,341

Correlating the complex of abietadiene and α2- antiplasmin with Ligplotanalysis [67]confirmed binding of abietadiene at one of the active binding site residues of α2- AP via H-bonding (residue no 1 which is proline) **{Figure 3 (A)}.** Also**,** abietadiene interacts with antithrombin III at C30 which also lies within the active site of protein {**Figure 3 (B)}.**

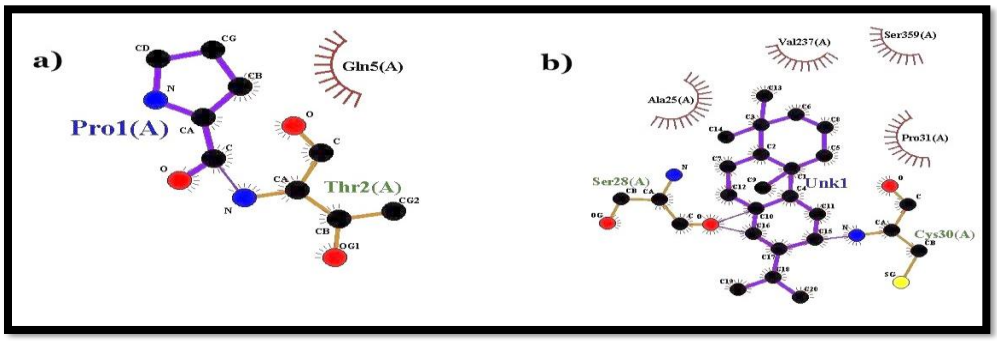

Figure 3`(a) Ligplot of abietadiene with α2-antiplasmin showing H-bonds between ligand and residue no 1 and 2 of α2-antiplasmin (b) Ligplot of abietadiene with antithrombin III showing H-bonds between ligand and residue no 28 and 30 of antithrombin III

3.5 Molecular Dynamics Simulations

MD simulation was carried out with the ligand protein complex with the least binding energy attained after performing molecular docking of each ligand. Interaction modes by 300 ns of complexes (Figure 4).MD simulations (green structures) and docking results (dark gray structures) of every molecule are demonstrated for comparison. MD simulations indicated that although there may be alterations in orientation of benzene rings present at the terminal ends of compounds, the trimethoxybenzene group

remains inside the groove. Figure 5 also indicated that barring compound number 19 and 26**,** all other compounds are bundled into the groove. Furthermore, it was also detected that 25, 21 and 22 compounds were drawn into the groove. In most cases, results obtained after MD simulations were coherent to the results retrieved after docking. Nonetheless, few differences were detected when bonding profiles and energy levels were evaluated.

RMSD calculation

Mass weighted RMSD analysis of 300 ns MD simulation of all complexes is depicted in figure 4. Altogether, RMSD values of all complexes was found to be 2-4 A° and they attained an equilibrium state. The complete set of compounds gave lesser RMSD values than those depicted in anticholinergic drug of tacrine. Considering this perspective, we can state that compounds.

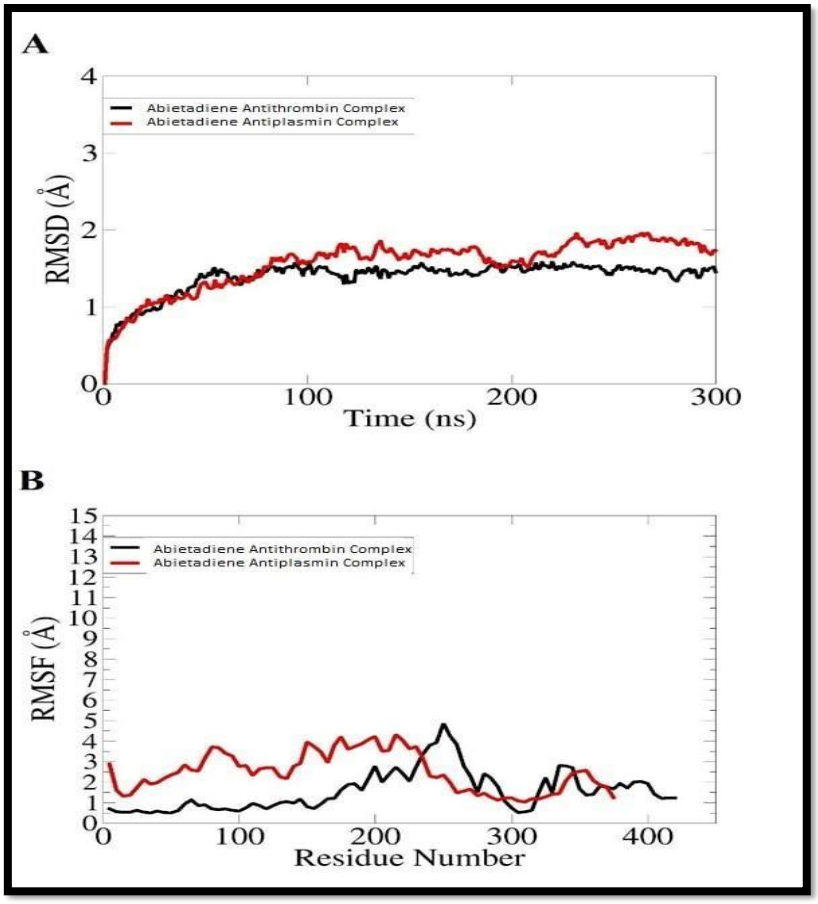

Figure 4: RMSF and RMSD values of Abietadiene-Antithrombin complex and Abietadiene Antiplasmin complex RMSF calculation

Root mean square fluctuations (RMSF) are calculated to consider the average positions of an atom and its values for Cα atoms (Figure 4). An average RMSF of 0.42nm has been evaluated for all atoms in comparison with 0.37nm of the apo protein, thus,overall, a slight increase in RMSF has been observed. Residues residing C-terminus of the complex, forming the coiled structure, have shown the largest RMSF along with a region in domain 1A (near residue CYS342) around the region outlining the domain near the domain 1B interface. Overall, the largest fluctuation has been shown by domain 2A. A region around VAL484 also depicts higher RMSF on domain 2A (coil). Whereas, ASP374 and GLU375 (in ATP binding domain) show smaller RMSF of about 0.2nm. Some more rigid regions have been observed around residue 136 lying in between Stalk and 1B domain (around PRO234 and ASN388).

MM/PBSA- MM/GBSA calculations

MM/PBSA calculations helped to unravel the MD simulations and energy changes within the complex. All the polar, non-polar, Vander Waals, dispersion and electrostatic energies calculated along with their standard errors, for 10 different compounds (Table 5). A strong interaction of compounds(-ΔG) has been observed with AChE and molecules showing the lowest binding energies as compared to others include 21 (-18.82 ± 0.7 kcal/mol), 22 (-16.31 ± 1.5 kcal/mol) and 19 (-14.08 ± 1.3 kcal/mol), quite similar to docking results (with a slight variation in calculated binding energies, though ranking remains the same).

Table 5:Energy Parameters of Abietadiene- Antiplasmin complex and Abietadiene-Antithrombin complex

Energy Parameter	Abietadiene-Antiplasmin complex	Abietadiene-Antithrombin complex
MM-GBSA		
Van der Waals Energy	-50.44	-51.26
Electrostatic Energy	-15.38	-18.00
Total Gas Phase Energy	20.38	18.44
Net Energy of System	-45.44	-50.82
MM-PBSA		
Van der Waals Energy	-50.44	-51.26
Electrostatic Energy	-15.38	-18.00
Total Gas Phase Energy	21.56	25.14
Net Energy of System	-44.26	-44.12

DISCUSSION

Secondary metabolites present in crude extracts of medically relevant plants are renowned for their beneficial roles [44]. *P.roxburghii,* natively known as Chir pine, is an indigenous plant of Himalayan region of Pakistan [69]. All of its parts including wood, resins, gum, seeds, oil, needles and barks have been employed in the management of numerous ailments[70]. Moreover, it is a valuable source of xanthones, flavonoids and terpenoids [71].

Abietadiene is a diterpene resin acid present in *P.roxburghii* [51,52]. It is more commonly recognized as being an intermediate compound in the cyclical biosynthesis of abietic acid. The enzyme responsible for this whole reaction goes by the name of abietadiene synthase [72]. Although multiple studies have been done on abietic acid and its multiple activities including anti-inflammatory activity by virtue of its lipoxygenase inhibitory action [73], osteoprotective effect due to its ability to repress synthesis of osteoclasts which in turn is due to abietic acid's ability to suppress activation of nuclear factor-kappa B ligand (RANKL)receptor [74]. Still other biomedical functions include anticonvulsant [75], antimicrobial [76], and 5α reductase inhibition activity which leads to its role in management of benign prostatic hyperplasia [77], among others. But abietadiene has been away from the limelight and in this study using *in silico* models, we have studied modulatory effect of abietadiene on anticoagulant pathway with a view that if purified, it can be used in the management of cold-induced injuries including frost-bite injuries.

Antithrombin III, a protease inhibitor , able to inactivate its biological targets which include factor IIa, IXa, Xa, XIa and factor XIIathus managing the whole clotting cascade [78]. Also, Human Alpha 2 antiplasmin (α2-antiplasmin aka α2-plasmin inhibitor aka α2AP) is the chief physiological inhibitor of plasmin [79]. α2AP belonging to the serine protease inhibitor family and accomplishes its task by covalent binding to plasmin and creating inert covalent complexes [80]. Various studies have reported the enhanced tPA mediated thrombolysis via inhibition of α2A[81]and thus can be a potential target**(Figure 5)**.

Plasmin-antiplasmin system plays a pivotal role he plasmin–antiplasmin system holds a key position in blood fibrinolysis and coagulation [82]. Two principal physiological activators of plasminogen exists namely urokinase-type plasminogen activator (uPA) and tissue-type plasminogen activator (tPA); whereas inhibition of plasminogen falls chiefly on the shoulders of antiplasmin and to some degree

on generic protease inhibitor α2-macroglobulin (α2M) **(Figure 5)**[83]. Human Alpha 2 antiplasmin (α2-antiplasmin aka α2-plasmin inhibitor aka α2AP) is the chief physiological inhibitor of plasmin [79]. α2AP belonging to the serine protease inhibitor family, accomplishes its task by covalent binding to plasmin and creating inert covalent complexes [80]. It has a considerably long C-terminal domain with a lysine residue occupying its terminal end and it is this lysine residue that serves as a secondary binding site of free circulating plasmin whose lysine binding site mediates this binding. This biding site is located in the kringle domain of plasmin [84]. Attempts have been made to enhance tPA mediated thrombolysis via inhibition of α2AP. Singh *et al* [81]managed to enhance tPA-mediated thrombolysis through the usage of a neutralizing antibody that specifically targets α2AP (α2AP-I) and induces an efficient inhibition after.

CONCLUSION

Present study concluded that abietadiene from *P.roxburghii*, if extracted and purified can be used as an adjuvant in the thrombolytic management of frostbite and can play a role in minimizing the incidences of amputation that occur due to intravascular thrombosis. Further studies encompassing the purified form of abietadiene can further enhance its chances of being used as an adjuvant therapy in the management of severe frostbite injury on the spot and during evacuation to a tertiary care hospital.

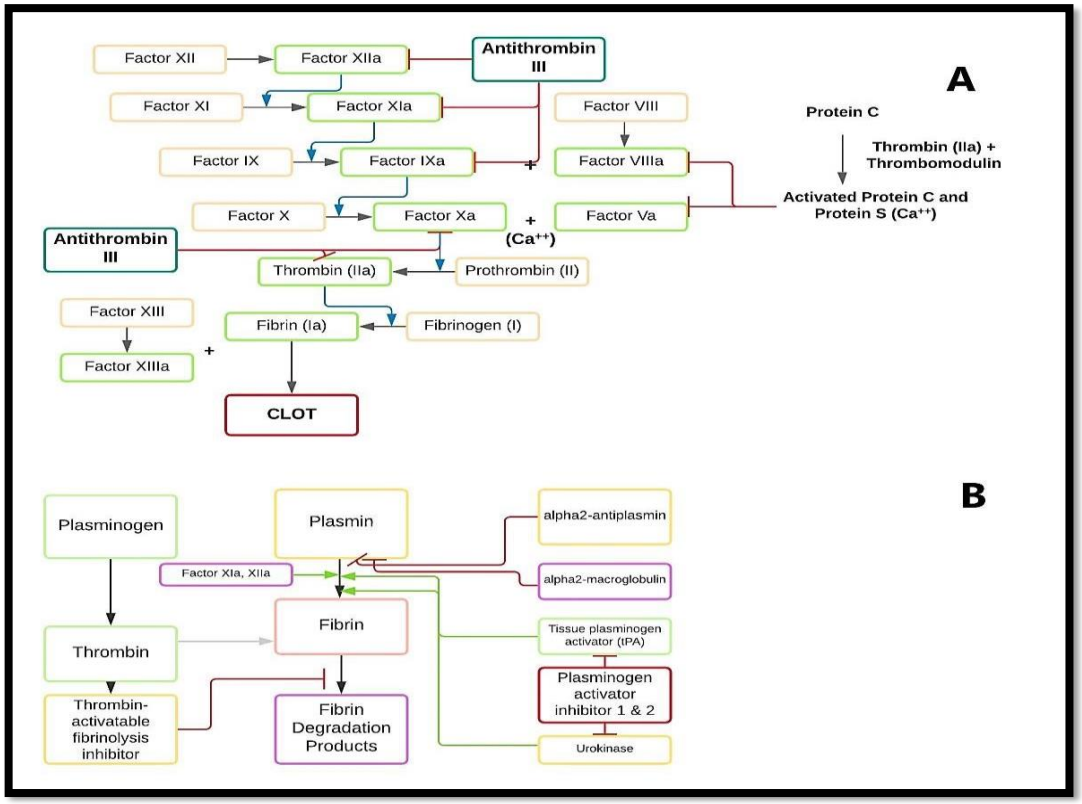

Figure 5:Schematic representation for intrinsic clotting pathway and the inhibitory role of Antithrombin III (A);Fibrinolytic pathway and the role of α2-antiplasmin in stabilizing the clot by inhibiting Plasmin(B); [85,86]

FUNDED BY

Present course of work was funded by HEC, Pakistan byNRPU grant No:8175.

ACKNOWLEDGMENT

Authors highly acknowledge the Higher Education Commission (HEC) Pakistan as a part of National Research Program for Universities Project (NRPU- 8715). Moreover, this work was impossible

without the cooperation and contribution of Pakistan Armed forces for their support for the collection of plants from Minimerg Pakistan.

SUPPLEMENTARY DATA: Abramov [50]

Table used for histological scoring of healing of wound

Variable	Score			
	0	**1**	**2**	**3**
Acute inflammation	None	Scant	Moderate	Abundant
Chronic inflammation	None	Scant	Moderate	Abundant
Granulation tissue amount	None	Scant	Moderate	Abundant
Granulation tissue/ fibroblast maturation	Immature	Mild maturation	Moderate maturation	Fully matured
	None	Scant	Moderate	Abundant
Collagen deposition	None	Partial	Complete but immature or thin	Complete and mature
Reepithelialization	None	Up to five vessels per HPF	6—10 vessels per HPF	More than 10 vessels per HPF

REFERENCES

1. Imray CHE, Oakley EHN. Cold still kills: cold-related illnesses in military practice freezing and non-freezing cold injury. *J R Army Med Corps*. 2005;151(4):218-222.
2. Imray CHE, Richards P, Greeves J, Castellani JW. Nonfreezing cold-induced injuries. *J R Army Med Corps*. 2011;157(1):79-84.
3. Yasir M, Nawaz A, Ghazanfar S, et al. Anti-bacterial activity of essential oils against multidrugresistant foodborne pathogens isolated from raw milk. Braz J Biol. 2022;84:e259449.
4. Nguyen CM, Chandler R, Ratanshi I, Logsetty S. Frostbite. In: Jeschke MG, Kamolz LP, Sjöberg F, Wolf SE, eds. *Handbook of Burns Volume 1: Acute Burn Care*. Springer International Publishing; 2020:529-547.
5. Sial N, Saeed S, Ahmad M, Hameed Y, Rehman A, Abbas M, Asif R, Ahmed H, Hussain MS,
6. Rehman JU, Atif M, Khan MR. Multi-Omics Analysis Identified TMED2 as a Shared Potential Biomarker in Six Subtypes of Human Cancer. Int J Gen Med. 2021 Oct 21;14:7025-7042
7. Bruen KJ, Ballard JR, Morris SE, Cochran A, Edelman LS, Saffle JR. Reduction of the Incidence of Amputation in Frostbite Injury with Thrombolytic Therapy. *Arch. Surg*. 2007;142(6):546-553.
8. Mao J, Huang X, Okla MK, et al. Risk Factors for TERT Promoter Mutations with Papillary
9. Thyroid Carcinoma Patients: A Meta-Analysis and Systematic Review. Comput Math Methods
10. Med. 2022;2022:1721526
11. Meyer AS, Johansson PI, Kjaergaard J, et al. Endothelial Dysfunction in Resuscitated Cardiac Arrest (ENDO-RCA): Safety and efficacy of low-dose Iloprost, a prostacyclin analogue, in addition to standard therapy, as compared to standard therapy alone, in post-cardiac-arrest-syndrome patients. *Am. Heart J.* 2020;219:9-20.
12. SHMT2 is associated with tumor purity, CD8+ T immune cells infiltration, and a novel therapeutic target in four different human cancers
13. Zhang L, Sahar AM, Li C, et al. A detailed multi-omics analysis of GNB2 gene in human cancers. Braz J Biol. 2022;84:e260169.
14. Stock G, Müller B, Krais T, Schillinger E. Iloprost, a stable analogue of PGI2: clinical results and pathophysiological considerations. *Adv. Prostaglandin Thromboxane Leukot. Res.* 1991;21:583-589.
15. Ullah L, Hameed Y, Ejaz S, et al. Detection of novel infiltrating ductal carcinoma-associated BReast CAncer gene 2 mutations which alter the deoxyribonucleic acid-binding ability of BReast CAncer gene 2 protein. J Cancer Res Ther. 2020;16(6):1402-1407.

16. Gusdon AM, Thompson CB, Quirk K, et al. CSF and serum inflammatory response and association with outcomes in spontaneous intracerebral hemorrhage with intraventricular extension: an analysis of the CLEAR-III Trial. *J. Neuroinflammation.*2021;18(1):1-11.
17. Spronk E, Sykes G, Falcione S, et al. Hemorrhagic transformation in ischemic stroke and the role of inflammation. *Front. Neurol.* 2021;12:661955.
18. Jickling GC, Liu D, Stamova B, et al. Hemorrhagic transformation after ischemic stroke in animals and humans. *J Cereb Blood Flow Metab*. 2014;34(2):185-199.
19. Vandenbroucke RE, Libert C. Is there new hope for therapeutic matrix metalloproteinase inhibition? *Nat Rev Drug Discov*. 2014;13(12):904-927.
20. Saleem S, Wang D, Zhao T, Sullivan RD, Reed GL. Matrix metalloproteinase-9 expression is enhanced by ischemia and tissue plasminogen activator and induces hemorrhage, disability and mortality in experimental stroke. *Neuroscience*. 2021;460:120-129.
21. Qiu M, Huang S, Luo C, et al. Pharmacological and clinical application of heparin progress: An essential drug for modern medicine. *Biomed. Pharmacother.* 2021;139:111561.
22. Furie B, Furie BC. Mechanisms of Thrombus Formation. *NEJM.* 2008;359(9):938-949.
23. Silberberg M. The causes and mechanism of thrombosis. *Physiol. Rev*. 1938;18(2):197-228.
24. Mackman N. Triggers, targets and treatments for thrombosis. *Nature*. 2008;451(7181):914-918. 22. Bansal A, Gupta P, Singh H, et al. Gastrointestinal complications in acute and chronic pancreatitis. *JGH Open*. 2019;3(6):450-455.
25. Daley MJ, Murthy MS, Peterson EJ. Bleeding risk with systemic thrombolytic therapy for pulmonary embolism: scope of the problem. *Ther. Adv. Drug Saf*. 2015;6(2):57-66.
26. Ageno W, Gallus AS, Wittkowsky A, Crowther M, Hylek EM, Palareti G. Oral anticoagulant therapy: Antithrombotic Therapy and Prevention of Thrombosis, 9th ed: American College of Chest Physicians Evidence-Based Clinical Practice Guidelines. *Chest*. 2012;141(2 Suppl):e44S-e88S.
27. Weitz JI. New oral anticoagulants: a view from the laboratory. *Am. J. Hematol* .2012; 87(S1):S133-S136.
28. Jamshidi-Kia F, Lorigooini Z, Amini-Khoei H. Medicinal plants: Past history and future perspective. *J. HerbMed Pharmacol.* 2018;7(1). Accessed October 26, 2021. http://eprints.skums.ac.ir/6978/
29. Matos J, Cardoso C, Bandarra NM, Afonso C. Microalgae as healthy ingredients for functional food: a review. *Food & function*. 2017;8(8):2672-2685.
30. Akram M, Rashid A. Anti-coagulant activity of plants: mini review. *J Thromb Thrombolysis*. 2017;44(3):406-411.
31. Ramjan A, Hossain M, Runa JF, Md H, Mahmodul I. Evaluation of thrombolytic potential of three medicinal plants available in Bangladesh, as a potent source of thrombolytic compounds. *Avicenna J Phytomed*. 2014;4(6):430-436.
32. Jakaria Md, Islam M, Shariful I Md, Belal Talu M, Dhar Clint C, Ibrahim M. Thrombolysis Potential of Methanol Extracts from the Five Medicinal Plants Leaf, Available in Bangladesh. *Pharmacologia*. 2017;8(2):78-82.
33. Kotlyakov V, Komarova A. *Elsevier's Dictionary of Geography: In English, Russian, French, Spanish and German*. Elsevier; 2006.
34. Bisht M, Sekar K, Arya D. Diversity, utilization pattern, threat status and conservation of medicinal plants in great Himalayan national park, Himachal pradesh, western Himalaya. *APJR*. 2019;1.
35. Gautam T, Gautam P, Keservani R, Sharma A. Phytochemical screening and wound healing potential of Cuscuta reflexa. *J. Chin. Pharm. Sci.*2015;24(5):292-302.
36. Man R, Samant S. Diversity, indigenous uses and conservation status of medicinal plants in Manali wildlife sanctuary, North Western Himalaya. *IJTK.* 2011;10(3):439-459.
37. Secim-Karakaya P, Saglam-Metiner P, Yesil-Celiktas O. Antimicrobial and wound healing properties of cotton fabrics functionalized with oil-in-water emulsions containing Pinus brutia

bark extract and Pycnogenol® for biomedical applications. *Cytotechnology*. 2021;73(3):423-431.
38. Shankar, Devkota S, Paudel K, et al. Investigation of antioxidant and anti-inflammatory activity of roots of *Rumex nepalensis. WJPPS*. 2015;4:582-589.
39. Gupta B, Dass B. Composition of herbage in *Pinus roxburghii* Sargent stands: basal area and importance value index. *Casp. J. Environ. Sci.* 2007;5(2):93-98.
40. Siddiqui MF, Ahmed M, Wahab M, et al. Phytosociology of Pinus roxburghii Sargent (chir pine) in lesser Himalayan and Hindu Kush range of Pakistan. *Pak J Bot*. 2009;41(5):2357-2369.
41. Ahmed M, Husain T, Sheikh AH, Hussain SS, Siddiqui MF. Phytosociology and structure of Himalayan forests from different climatic zones of Pakistan. *Pak J Bot*. 2006;38(2):361.
42. Hassan A, Amjid I. Gas chromatography-mass spectrometric studies of essential oil of *Pinus roxburghii* stems and their antibacterial and antifungal activities. *J. Med. Plant Res.* 2009;3(9):670673.
43. Salem MZM, Ali HM, Basalah MO. Essential Oils from Wood, Bark, and Needles of *Pinus roxburghii*Sarg. from Alexandria, Egypt: Antibacterial and Antioxidant Activities. *Bioresources*. 2014;9(4):7454-7466.
44. Labib RM, Youssef FS, Ashour ML, Abdel-Daim MM, Ross SA. Chemical Composition of *Pinus roxburghii* Bark Volatile Oil and Validation of Its Anti-Inflammatory Activity Using Molecular Modelling and Bleomycin-Induced Inflammation in Albino Mice. *Molecules*. 2017;22(9):1384.
45. Farooq Z, Iqbal Z, Mushtaq S, Muhammad G, Iqbal MZ, Arshad M. Ethnoveterinary practices for the treatment of parasitic diseases in livestock in Cholistan desert (Pakistan). *J Ethnopharmacol*. 2008;118(2):213-219.
46. Sajid A, Manzoor Q, Iqbal M, Tyagi AK, Sarfraz RA, Sajid A. *Pinus roxburghii*essential oil anticancer activity and chemical composition evaluation. *EXCLI J*. 2018;17:233-245.
47. Sharma A, Sharma L, Goyal R. GC/MS Characterization, in-vitro Antioxidant, Antiinflammatory and Antimicrobial Activity of Essential Oils from Pinus Plant Species from Himachal Pradesh, India. *JEOBP*.2020;23(3):522-531.
48. Safaeian L, Zolfaghari B, Assarzadeh N, Ghadirkhomi A. Antioxidant and Anti-hyperlipidemic Effects of Bark Extract of *Pinus eldarica* in Dexamethasone-induced Dyslipidemic Rats. *J Adv Med Biomed Res.*2019;27(125):49-56.
49. Tripathi A, Misra K. Molecular docking: A structure-based drug designing approach. *JSM Chem*. 2017;5(2):1042-1047.
50. Ben Sghaier M, Louhichi T, Hakem A, Ammari Y. Chemical investigation of polar extracts from *Ruta chalpensis* L. growing in Tunisia: Correlation with their antioxidant activities. *J. New Sci.* 2018;49(4): 2971-2978.
51. Jijith US, Jayakumari S. An Apparatus for the determination of rat paw Edema during In vivo Evaluation of Anti-inflammatory agents. *Research J Pharm and Tech*. 2020;13(5):1-3.
52. Abramov Y, Golden B, Sullivan M, et al. Histologic characterization of vaginal vs. abdominal surgical wound healing in a rabbit model. *Wound Repair Regen.*2007;15(1):80-86.
53. Satyal P, Paudel P, Raut J, Deo A, Dosoky NS, Setzer WN. Volatile constituents of *Pinus roxburghii* from Nepal. *Pharmacognosy Res*. 2013;5(1):43-48.
54. Tsvetkov DE, Kumar R, Devrani R, et al. Chemical constituents of the extracts of the knotwood of *Pinus roxburghii* Sarg. and their antioxidant activity. *Russ. Chem. Bull.* 2019;68(12):2298-2306. 53. Kaushik P, Kaushik D, Khokra SL. Ethnobotany and phytopharmacology of *Pinus roxburghii*Sargent: a plant review. *J. Integr. Med.*2013;11(6):371-376.
55. Qadir M, Shah WA, Banday JA. GC-MS analysis, antibacterial, antioxidant and anticancer activity of essential oil of *Pinus roxburghii* from Kashmir, India. *Int J Res Pharm Chem*. 2014;4(1):228-232.
56. Hamad AMA, Ates S, Olgun Ç, Gur M. Chemical Composition and Antioxidant Properties of Some Industrial Tree Bark Extracts. *BioResources*. 2019;14(3):5657-5671.

57. Lipinski CA. Lead-and drug-like compounds: the rule-of-five revolution.*Drug Discov. Today Technol.* 2004;1(4):337-341.
58. Lipinski CA, Lombardo F, Dominy BW, Feeney PJ. Experimental and computational approaches to estimate solubility and permeability in drug discovery and development settings. *Adv. Drug Deliv. Rev.* 1997;23(1-3):3-25.
59. Daina A, Michielin O, Zoete V. SwissADME: a free web tool to evaluate pharmacokinetics, drug-likeness and medicinal chemistry friendliness of small molecules. *Sci Rep*. 2017;7(1):42717. 59. Kim S, Chen J, Cheng T, et al. PubChem in 2021: new data content and improved web interfaces. *Nucleic Acids Res*. 2021;49(D1):D1388-D1395.
60. The UniProt Consortium. UniProt: a worldwide hub of protein knowledge. *Nucleic Acids Res*. 2019;47(D1):D506-D515.
61. Waterhouse A, Bertoni M, Bienert S, et al. SWISS-MODEL: homology modelling of protein structures and complexes. *Nucleic Acids Res*. 2018;46(W1):W296-W303.
62. Pettersen EF, Goddard TD, Huang CC, et al. UCSF Chimera—a visualization system for exploratory research and analysis.*J. Comput. Chem.* 2004;25(13):1605-1612.
63. Ramachandran S, Kota P, Ding F, Dokholyan NV. Automated minimization of steric clashes in protein structures. *Proteins*. 2011;79(1):261-270.
64. Liu Y, Grimm M, Dai W tao, Hou M chun, Xiao ZX, Cao Y. CB-Dock: a web server for cavity detection-guided protein–ligand blind docking. *Acta Pharmacol Sin*. 2020;41(1):138-144.
65. Yang J, Roy A, Zhang Y. Protein–ligand binding site recognition using complementary binding-specific substructure comparison and sequence profile alignment. *Bioinformatics*. 2013;29(20):2588-2595.
66. Porollo A, Meller J. Prediction-based fingerprints of protein-protein interactions. *Proteins*. 2007;66(3):630-645.
67. Laskowski RA, Swindells MB. LigPlot+: multiple ligand-protein interaction diagrams for drug discovery. *J Chem Inf Model*. 2011;51(10):2778-2786.
68. Burmaoglu S, Kazancioglu EA, Kazancioglu MZ, et al. Synthesis, molecular docking and some metabolic enzyme inhibition properties of biphenyl-substituted chalcone derivatives. *J. Mol. Struct.* 2022;1254:132358.
69. Shuaib M, Ali M, Naquvi KJ. New abietatriene-type diterpenes linked with lanostenes from oleo-resin of *Pinus roxburghii* Sarg. *Acta Pol Pharm*. 2014;71(1):205-212.
70. Thapa R, Upreti A, Pandey BP. Chemical profiling and biological activity analysis of cone, bark, and needle of *Pinus roxburghii* collected from Nepal. *J. Intercult.*
71. *Ethnopharmacol.*2018;1(1):66-75.
72. Kaushik P, Lal S, Rana AC, Kaushik D. GC-MS analysis of bioactive constituents of *Pinus roxburghii Sarg.* (Pinaceae) from northern India. *Res. J. Phytochem.* 2014;8(2):42-46.
73. Trapp S, Croteau R. Defensive resin biosynthesis in conifers.*Annu. Rev. Plant Biol.* 2001;52(1):689-724.
74. Mane V. In-vitro Evaluation of Phytochemical Compounds for Their Potential Beneficial Effect in Immuno-Inflammatory Diseases. In: *Proceedings of International Conference on Drug Discovery (ICDD).*; 2020
75. Thummuri D, Guntuku L, Challa VS, Ramavat RN, Naidu VGM. Abietic acid attenuates RANKL induced osteoclastogenesis and inflammation associated osteolysis by inhibiting the NFKB and MAPK signaling. *J. Cell. Physiol*. 2019;234(1):443-453.
76. Talevi A, Cravero MS, Castro EA, Bruno-Blanch LE. Discovery of anticonvulsant activity of abietic acid through application of linear discriminant analysis. *Bioorg. Med. Chem. Lett*. 2007;17(6):1684-1690.
77. Ito Y, Ito T, Yamashiro K, et al. Antimicrobial and antibiofilm effects of abietic acid on cariogenic Streptococcus mutans. *Odontology*. 2020;108(1):57-65.
78. Roh SS, Park MK, Kim YU. Abietic acid from resina pini of Pinus species as a testosterone 5αreductase inhibitor. *J. Health Sci.* 2010;56(4):451-455.

79. Bedsted T, Swanson R, Chuang YJ, Bock PE, Björk I, Olson ST. Heparin and Calcium Ions Dramatically Enhance Antithrombin Reactivity with Factor IXa by Generating New Interaction Exosites. *Biochemistry*. 2003;42(27):8143-8152.
80. Abdul S, Leebeek FW, Rijken DC, Uitte de Willige S. Natural heterogeneity of α2-antiplasmin: functional and clinical consequences. *Blood*.2016;127(5):538-545.
81. Collen D, Wiman B. Fast-acting plasmin inhibitor in human plasma. *Blood*. 1978;51(4):563569.
82. Singh S, Houng A, Reed GL. Releasing the brakes on the fibrinolytic system in pulmonary emboli: unique effects of plasminogen activation and α2-antiplasmin inactivation. *Circulation*. 2017;135(11):1011-1020.
83. Gerber SS, Lejon S, Locher M, Schaller J. The human alpha(2)-plasmin inhibitor: functional characterization of the unique plasmin(ogen)-binding region. *Cell Mol Life Sci*. 2010;67(9):15051518.
84. Schaller J, Gerber SS. The plasmin–antiplasmin system: structural and functional aspects. *Cell Mol Life Sci*. 2011;68(5):785-801.
85. Urano T, Suzuki Y. Thrombolytic therapy targeting alpha 2-antiplasmin. *Circulation*. 2017;135(11):1021-1023.
86. Bauer KA, Nguyen-Cao TM, Spears JB. Issues in the diagnosis and management of hereditary antithrombin deficiency. *Ann Pharmacother*. 2016;50(9):758-767.
87. Plasminogen activator. In: *Wikipedia*.; 2021. Accessed January 3, 2022. https://en.wikipedia.org/w/index.php?title=Plasminogen_activator&oldid=1055120794